Inorg. Chem. **2008**, *47*, 1597−1606

Mononuclear, Dinuclear, and Hexanuclear Gold(I) Complexes with (aza-15-crown-5)Dithiocarbamate

Javier Arias, **Manuel Bardají**, **and Pablo Espinet***

IU CINQUIMA/Química Inorgánica, Facultad de Ciencias, Universidad de Valladolid, E-47071 Valladolid, Spain

Received November 15, 2007

The reactions of sodium (aza-15-crown-5)dithiocarbamate with [AuClL] precursors lead to mono-, di-, or hexanuclear derivatives depending on L. The homoleptic hexanuclear gold(I) cluster $[Au_6(S_2CNC_{10}H_{20}O_4)_6]$ is formed by displacement of the chloride and isocyanide ligands in $[AuCl(CN(2,6\text{-}Me_2C_6H_3))]$. X-ray diffraction studies show a novel geometry in gold cluster chemistry where the six gold atoms display a cyclohexane-like geometry in a chair conformation with Au−Au−Au angles of 117.028(9)°, two short gold−gold distances of 2.9289(5) Å, and bidentate bridging dithiocarbamate ligands. The molecular structure shows a crown of gold atoms surrounded by crown ethers. This derivative luminesces at 569 nm at room temperature in the solid state. A dinuclear isomer $[Au_2(S_2CNC_{10}H_{20}O_4)_2]$ had been reported previously and was obtained by reaction with $[AuCl(SMe_2)]$. The mechanism to obtain the hexanuclear derivative involves a mononuclear intermediate $[Au(S_2CNC_{10}H_{20}O_4)(CNR)]$ for which the X-ray structure shows a short gold−gold distance of 3.565 Å with the two molecules in an anti configuration. Phosphine gold(I) mononuclear derivatives $[Au(S_2CNC_{10}H_{20}O_4)(PR_3)]$ (R = Me, Ph, both characterized by X-ray diffraction) and dinuclear diphosphine derivatives $[\{Au(S_2CNC_{10}H_{20}O_4)\}_2(\mu\text{-P-P})]$ (P-P = dppm, bis(diphenylphosphinomethane); dppp, 1,3-bis(diphenylphosphinopropane); and dppf, 1,1′-bis(diphenylphosphinoferrocene)) are also reported. In the mononuclear complexes, the molecular structure confirms that the dithiocarbamato ligand is mainly acting as monodentate, with a second longer Au−S distance of 3.197 (PMe_3), 2.944(4) (PPh_3), and 2.968 Å (CNR). Three phosphine complexes are emissive at 562 (PMe_3), 528 (PPh_3), and 605 nm (dppm), at 77 K. X-ray diffraction studies of the dppm derivative show gold−gold intramolecular contacts of 3.0972(9) Å (3.2265(10) Å for a second independent molecule) and basically monodentate coordination of the dithiocarbamato ligands. All the complexes extract sodium and potassium salts from aqueous solutions. The diphosphine derivatives are noticeably better extractors than the monophosphino derivatives, mainly for potassium salts.

Introduction

The synthesis of closed-shell polynuclear gold(I) derivatives has attracted considerable attention in recent years because of the presence of short gold−gold distances, which have been attributed to correlation effects reinforced by relativistic effects and electrostatic contributions.[1,2] Many of these derivatives are luminescent in the visible region.[3,4] Besides, thiolate gold(I) derivatives have been extensively studied for their pharmacological applications.[5,6]

The use of dithiocarbamate and other S ligands in gold chemistry has been reviewed.[5,7] Homoleptic dithiocarbamate derivatives are dimers with short intramolecular Au···Au distances, which possess a strong propensity to aggregate to form chains with short intermolecular Au···Au contacts,[8–12]

* Author to whom correspondence should be addressed. E-mail: espinet@qi.uva.es.

(1) Pyykkö, P. *Angew. Chem., Int. Ed.* **2004**, *43*, 4412.
(2) Runeberg, N.; Schütz, M.; Werner, H. J. *J. Chem. Phys.* **1999**, *110*, 7210.
(3) Schmidbaur, H. *Gold Bull.* **2000**, *33*, 3.
(4) Roundhill, D. M.; Fackler, J. P., Jr. *Optoelectronic Properties of Inorganic Compounds*; Plenum Press Ed.: New York and London, 1998; p 195.
(5) Mohamed, A. A.; Abdou, H. E.; Chen, J.; Bruce, A. E.; Bruce, M. R. M. *Comments Inorg. Chem.* **2002**, *23*, 321.
(6) Shaw, C. F., III. *Gold: Progress in Chemistry, Biochemistry, and Technology*; Schmidbaur, H., Ed.; John Wiley & Sons: Chichester, U.K., 1999; p 259.
(7) Fackler, J. P., Jr.; van Zyl, W. E.; Prohoda, B. *Gold: Progress in Chemistry, Biochemistry, and Technology*; Schmidbaur, H., Ed.; John Wiley & Sons: Chichester, U.K., 1999; p 795.
(8) Åkeström, S. *Ark. Kemi* **1959**, *14*, 387.

10.1021/ic702252j CCC: $40.75
Published on Web 02/01/2008

Scheme 1

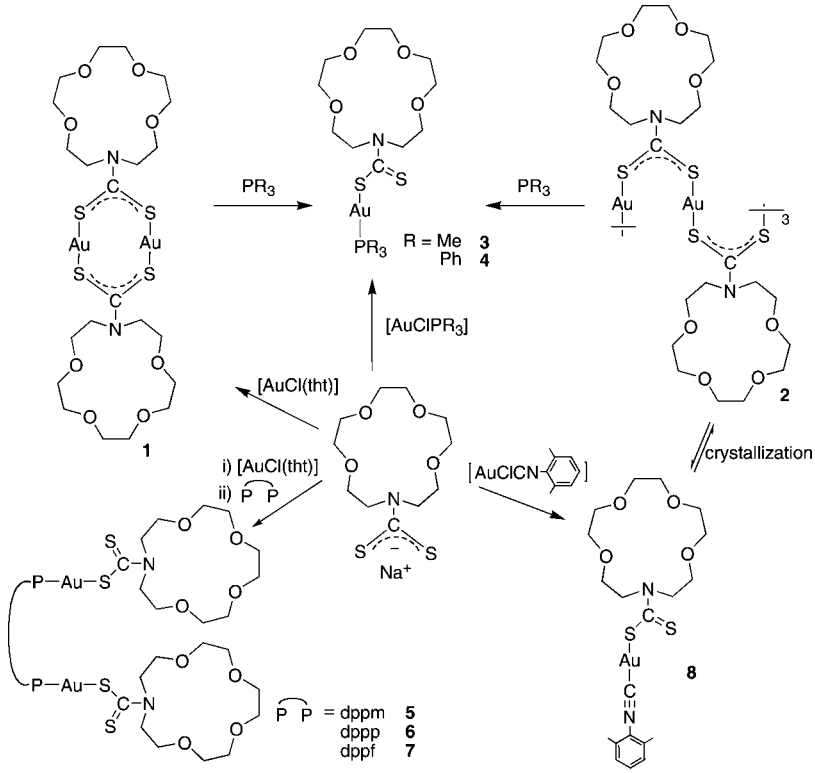

and show luminescence that has been attributed to these contacts.[12] The dinuclear gold complex with (aza-15-crown-5)dithiocarbamate (**1**) was recently reported and displays short intramolecular Au···Au distances, but no intermolecular Au···Au interactions. Consistently, the compound is not emissive.[13] We report here a hexanuclear Au(I) cluster, luminescent at room temperature, which is an isomer of **1**, and a luminescent intermediate derivative, [Au(S_2CN-crown)(CNR)], from which the hexanuclear isomer is formed. We also report five mononuclear mono- and diphosphine dithiocarbamato gold derivatives, three of which are luminescent at 77 K.

Results and Discussion

Synthesis and Characterization. The previously reported homoleptic dinuclear derivative **1** and the new gold dithiocarbamate derivatives **2**−**7** are prepared according to Scheme 1. Compounds **1** and **2** react rapidly with phosphines to give the same complexes **3** and **4**, suggesting that **1** and **2** only differ in the bridging mode of the dithiocarbamate group. Similarly, in situ prepared **1** reacts with diphosphines, affording the dinuclear derivatives with bridging diphosphines **5**−**7**. The isolation of crystals of the elusive intermediate **8** is discussed later. (Crystallographic data, in the form of a CIF file, are provided as Supporting Information.)

Complexes **1**−**7** are air- and moisture-stable, yellow (**1**−**6**) or orange (**7**) solids at room temperature that were characterized by elemental analysis, IR and NMR spectroscopy, and single-crystal X-ray diffraction for **2**−**5**. The main features observed in the IR spectra are (a) disappearance of the Au−Cl and (for **2**) the isocyanide vibrations of the starting material and (b) the presence of typical dithiocarbamate bands for ν(C═N) around 1480 cm^{-1} and ν(C−S) around 990 cm^{-1}; the latter is split for the phosphino complexes **3**−**7**, as expected for a mostly monodentate bound ligand.[14] The ^{1}H NMR dithiocarbamate resonances are quite insensitive to coordination. The ^{31}P{^{1}H} NMR spectra of complexes **3**−**7** show a singlet at −6.3, 36.9, 28.9, 29.3, and 30.4 ppm, respectively. Complex **2** is insoluble in common organic solvents, which precluded its NMR characterization.

X-Ray Crystal Structure Determination of Compounds 2−5 and 8. Crystal Structure of Complex 2. All the previously reported homoleptic dithiocarbamato gold(I) derivatives are dimers with very short intramolecular gold(I)−gold(I) distances of 2.75–2.80 Å (for instance, 2.7820(5) Å for the (aza-15-crown-5)dithiocarbamate), which aggregate to form chains with short intermolecular Au···Au contacts around 3 Å, with the planes of the dimers perpendicularly arranged.[8−12] Only the (aza-15-crown-5)dithiocarbamate dimer **1** does not form chains, probably because the formation of C−H···O weak nonclassical hydrogen bridges between the crown ether unit is incompatible with the formation of chains.[13]

The structure of the complex **2**, established by X-ray diffraction, is shown in Figure 1, with selected bond lengths and angles in Table 1. The molecule turns out to be an isomer

(9) Hesse, R.; Jennische, P. *Acta Chem. Scand.* **1972**, *26*, 3855.
(10) Heinrich, D. D.; Wang, J. C.; Fackler, J. P. *Acta Crystallogr., Sect. C: Cryst. Struct. Commun.* **1990**, *46*, 1444.
(11) Bishop, P.; Marsh, P.; Brisdon, A. K.; Brisdon, B. J.; Mahon, M. F. *J. Chem. Soc., Dalton Trans.* **1998**, 675.
(12) Mansour, M. A.; Connick, W. B.; Lachicotte, R. J.; Gysling, H. J.; Eisenberg, R. *J. Am. Chem. Soc.* **1998**, *120*, 1329.
(13) Tzeng, B.-C.; Liu, W.-H.; Liao, J.-H.; Lee, G.-H.; Peng, S.-H. *Cryst. Growth Des.* **2004**, *4*, 573.
(14) Bonati, F.; Ugo, R. *J. Organomet. Chem.* **1967**, *10*, 257.

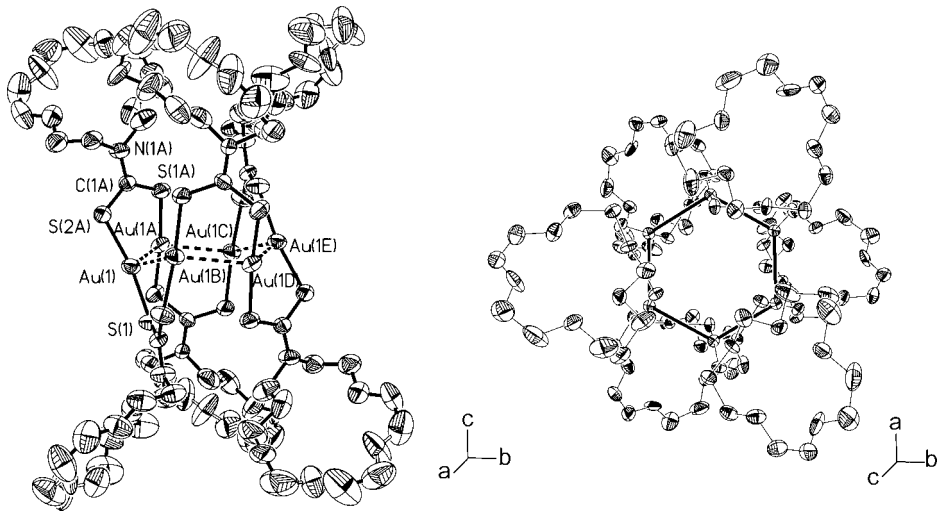

Figure 1. Two different views of **2**. Displacement ellipsoids are at the 50% (left) or 20% (right) probability level (H atoms omitted for clarity).

Table 1. Selected Bond Lengths [Å] and Angles [deg] for Complex **2**[a]

Au(1)−S(2A)	2.286(3)	S(2A)−Au(1)−S(1)	170.53(10)
Au(1)−S(1)	2.291(3)	S(2A)−Au(1)−Au(1A)	87.44(7)
Au(1)−Au(1A)	2.9289(5)	S(1)−Au(1)−Au(1A)	96.69(7)
Au(1)−Au(1B)	2.9289(5)	S(2A)−Au(1)−Au(1B)	97.69 (8)
S(1)−C(1)	1.729(9)	S(1)−Au(1)−Au(1B)	88.05(7)
S(2)−C(1)	1.720(10)	Au(1A)−Au(1)−Au(1B)	117.028(9)
C(1)−N(1)	1.320(11)	C(1)−S(1)−Au(1)	110.4(3)
N(1)−C(2)	1.478(12)	N(1)−C(1)−S(2)	116.8(7)
N(1)−C(11)	1.602(15)	N(1)−C(1)−S(1)	117.9(7)
C(2)−C(3)	1.488(14)	S(2)−C(1)−S(1)	125.4(6)
C(3)−O(1)	1.382(13)	C(1)−N(1)−C(2)	122.8(8)
O(1)−C(4)	1.349(14)	C(1)−N(1)−C(11)	121.8(8)

[a] Symmetry transformations used to generate equivalent atoms. A: $y - 1/3, -x + y + 1/3, -z + 7/3$. B: $x - y + 2/3, x + 1/3, -z + 7/3$.

of the reported dinuclear complex **1**.[13] It is a hexanuclear complex with the six gold atoms arranged in a perfect chairlike conformation (Figure 1), held together by a zigzag system of bridging dithiocarbamates. The S(2A)−Au(1)−S(1) angle is 170.53(10)° and corresponds to a slightly distorted linear geometry for the gold atom. The hexagold core displays Au−Au−Au angles of 117.028(9)°, and each gold is connected to two neighbors at short gold−gold distances of 2.9289(5) Å. The next gold neighbors in the hexagold core are at a distance of 4.995 Å, and the farthest one is at 5.791 Å. The shortest intermolecular gold−gold distance is 9.157 Å.

Gold displays a rich cluster chemistry often involving $AuER_3^+$ units (E = P and As). The typical arrangement for Au_6 clusters is that of dimers of trinuclear derivatives, as in $[\{X(AuER_3)_3\}_2]^{n+}$ ($n = 2$, X = O, S, Se, and Te; $n = 0$, X = N).[15] A trigonal prismatic arrangement of six gold atoms formed by gold−gold interactions between two gold triangles ($n = 3 \times 2$) is also the structure of $[Au\{2\text{-PyN}{=}C(NH)Me\}]_n$.[16] To our knowledge, complex **2** is the first example of cyclohexane-like geometry in gold cluster chemistry. Recent theoretical studies predicted, for ligandless systems, that the lowest energy isomer for hexanuclear gold clusters should be planar.[1,17,18] In agreement with this prediction, in the reported structure for $[Au_6(S_2CC_6H_4(o\text{-}CH_3))_6]$,[19] which also has a zigzag system of bridging dithiocarboxylates, the six gold atoms of the central cluster are coplanar to within 0.14 Å. Thus, the chairlike structure observed for **2** is exceptional. A more detailed observation of the tridimensional molecular packing of **2** in the crystal gives hints for the origin of the chairlike arrangement of the gold cluster, as well as for the insolubility of the compound. As shown in Figure 1, the hexagold cluster is sandwiched between crown-ether layers, and the three crown ether rings above and below the gold cluster are disposed as the blades of a fan. It is this arrangement which pushes the sulfur atoms and, with them, the gold atoms away from coplanarity, overcoming the expected tendency to a planar arrangement of six gold atoms.

The folded arrangement of crown ethers has its origin in the formation of a tridimensional packing that allows for a closer intermolecular approximation of crown ethers in successive layers along the *c* axis (each molecule is sandwiched by two identical molecules), as well as in the same layer (each molecule is surrounded by six identical molecules) (Figure 2). The disorder of some crown ether atoms in the X-ray structure, and the non-observation of the corresponding H atoms, precludes an exact determination of all distances, but it can be calculated that there is a multitude of C···O distances shorter than 3.5 Å,[20] which could correspond to so-called C−H···O weak nonclassical hydrogen-bonding interactions. It is this extended network of interactions that would account for the insolubility of **2**. The

(15) Gimeno, M. C.; Laguna, A. *Silver and Gold in Comprehensive Coordination Chemistry II*; McCleverty, J. A., Meyer, T. J., Fenton, D. E., Eds.; Elsevier Pergamon: Oxford, U.K., 2004; Vol. 6, p 911.
(16) Bartolomé, C.; Carrasco-Rando, M.; Coco, S.; Cordovilla, C.; Espinet, P.; Martín-Álvarez, J. M. *Organometallics* **2006**, *25*, 2700.
(17) Olson, R. M.; Varganov, S.; Gordon, M. S.; Metiu, H.; Chretien, S.; Piecuch, P.; Kowalski, K.; Kucharski, S. A.; Musial, M. *J. Am. Chem. Soc.* **2005**, *127*, 1049.
(18) Bravo-Pérez, G.; Garzón, I. L.; Novaro, O. *THEOCHEM* **1999**, *493*, 225.
(19) Schuerman, J. A.; Fronczek, F. R.; Selbin, J. *J. Am. Chem. Soc.* **1986**, *108*, 336.
(20) Several C···O intermolecular distances in the range 3.3–3.5 Å, for each crown ether moiety, are found. In addition, there is a posible weak C3−H3A···S2 intermolecular contact (six per hexamer) connecting columns in the *xy* plane: 2.873 Å (H3A···S2) and 3.677 Å (C3−S2) and a C3H3AS2 angle of 140.80.

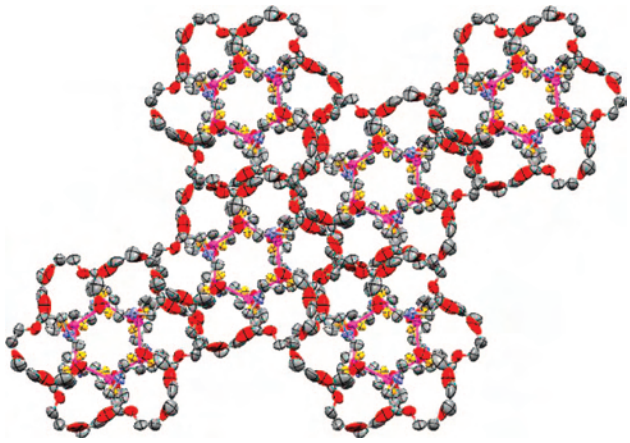

Figure 2. Crystal packing containing three layers, almost down the *c* axis. Displacement ellipsoids are at the 50% probability level.

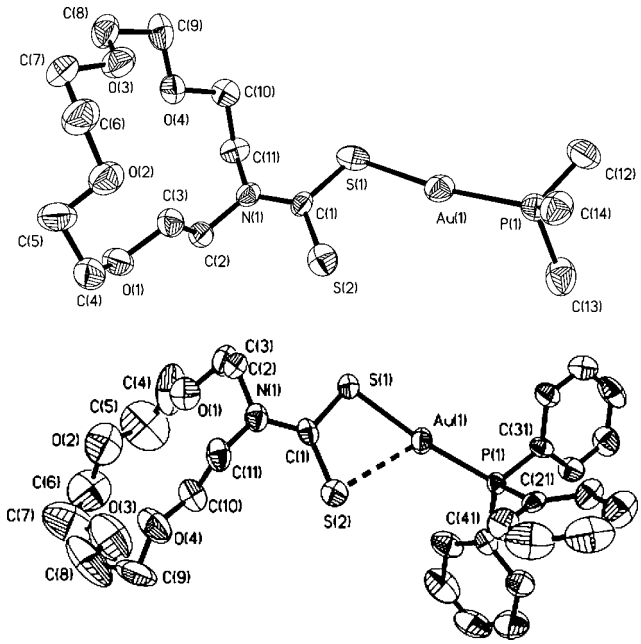

Figure 3. Structures of **3** (up) and **4** (down), showing displacement ellipsoids at the 50% probability level (H atoms and crystallization CH_2Cl_2 for 3 omitted for clarity).

Table 2. Selected Bond Lengths [Å] and Angles [deg] for Complex **3**

Au(1)−P(1)	2.247(2)	P(1)−Au(1)−S(1)	170.33(8)
Au(1)−S(1)	2.332(2)	C(12)−P(1)−C(13)	104.4(5)
S(1)−C(1)	1.751(8)	C(13)−P(1)−Au(1)	113.6(4)
C(1)−N(1)	1.321(10)	C(14)−P(1)−Au(1)	116.6(3)
C(1)−S(2)	1.696(8)	C(1)−S(1)−Au(1)	102.5(3)
N(1)−C(2)	1.472(11)	N(1)−C(1)−S(2)	123.2(6)
N(1)−C(11)	1.479(11)	N(1)−C(1)−S(1)	117.3(6)
C(2)−C(3)	1.516(11)	S(2)−C(1)−S(1)	119.5(4)

hexagonal tunnels apparently suggested by Figure 2 are somewhat deceptive, as the distances between the nonplanar crown ether rings are far too long (around 8 Å).

Crystal Structures of Complexes 3 and 4. The mononuclear structures of **3** and **4** were confirmed by X-ray diffraction studies and are shown in Figure 3. A selection of bond lengths and angles is given in Tables 2 and 3. The nonbonding shortest intermolecular Au/Au distances are 6.379 and 7.654 Å, for derivatives **3** and **4**, respectively.

Table 3. Selected Bond Lengths [Å] and Angles [deg] for Complex **4**

Au(1)−P(1)	2.253(3)	P(1)−Au(1)−S(1)	172.80(8)
Au(1)−S(1)	2.339(3)	S(2)−Au(1)−S(1)	66.91(10)
S(1)−C(1)	1.745(10)	C(21)−P(1)−Au(1)	111.0(3)
S(2)−C(1)	1.696(11)	C(1)−S(1)−Au(1)	96.7(4)
C(1)−N(1)	1.337(13)	N(1)−C(1)−S(2)	124.0(7)
N(1)−C(2)	1.450(14)	N(1)−C(1)−S(1)	117.6(8)
N(1)−C(11)	1.480(14)	S(1)−C(1)−S(2)	118.3(6)
C(2)−C(3)	1.50(2)	C(1)−N(1)−C(2)	123.0(9)

The gold atoms display in both complexes a slightly distorted linear geometry, with a P(1)−Au(1)−S(1) angle of 170.33(8)° for **3** and 172.80(8)° for **4**. The Au−P distance is 2.247(2) Å for **3** and 2.253(3) Å for **4**, close to others reported for this kind of derivative. The Au(1)−S(1) distance is 2.332(2) Å for **3** and 2.339(3) Å for **4**, slightly shorter than that in complex **2**. In complex **3**, the Au(1)−S(2) distance is 3.197 Å, while complex **4** displays a significantly different Au(1)−S(2) distance of 2.944(4) Å. Consistently, the dithiocarbamate ligand shows two different C−S bond lengths: one shorter at 1.696(8) Å (1.696(11) for **4**) for the dangling sulfur atom and one slightly longer at 1.751(8) Å (1.745(10) for **4**) for the coordinated one. The very dissimilar Au−S distances support the ditiocarbamate ligands being essentially monodentate, although the value of the longer distances suggests a weak contact between the gold atom and the dangling sulfur atom, as reported, for instance, for $[Au(S_2CNEt_2)(PPh_3)]$ with Au−S bond distances of 2.338 and 3.015 Å.[21] This possible weak interaction looks more plausible for **4**, which has more acceptor phosphine and shows a noticeably shorter Au(1)−S(2) distance.

Crystal Structure of Complex 5. Complex **5** crystallizes with two independent but rather similar molecules in the asymmetric unit. One molecule is shown in Figure 4, and a selection of bond lengths and angles is given in Table 4.

The P−Au−S angles (ranging from 168.89(11) to 176.31(10)°) confirm a linear geometry around the gold atoms, although slightly distorted for Au(2), Au(3), and Au(4). The main difference between the two independent molecules is the intramolecular Au−Au distance, 3.0972(9) Å for Au(1)−Au(2) and 3.2265(10) Å for Au(3)−Au(4),

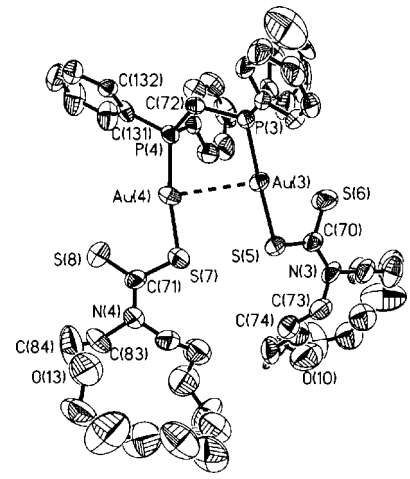

Figure 4. One of the two independent molecules of complex **5** in the crystal, showing displacement ellipsoids at the 50% probability level (H atoms omitted for clarity).

Table 4. Selected Bond Lengths [Å] and Angles [deg] for Complex **5**

Au(1)−P(1)	2.250(3)	Au(3)−P(3)	2.254(3)
Au(1)−S(1)	2.322(3)	Au(3)−S(5)	2.334(4)
Au(1)−Au(2)	3.0972(9)	Au(3)−Au(4)	3.2265(10)
Au(2)−P(2)	2.247(3)	Au(4)−P(4)	2.256(4)
Au(2)−S(3)	2.335(3)	Au(4)−S(7)	2.329(4)
S(1)−C(1)	1.758(11)	S(5)−C(70)	1.735(12)
S(2)−C(1)	1.662(13)	S(6)−C(70)	1.690(14)
C(1)−N(1)	1.324(12)	C(70)−N(3)	1.335(15)
S(3)−C(2)	1.743(11)	S(7)−C(71)	1.712(13)
S(4)−C(2)	1.669(13)	S(8)−C(71)	1.665(15)
C(2)−N(2)	1.348(15)	C(71)−N(4)	1.358(17)
N(2)−C(23)	1.459(16)	N(4)−C(83)	1.501(16)
P(1)−Au(1)−S(1)	176.31(10)	P(3)−Au(3)−S(5)	173.49(12)
P(1)−Au(1)−Au(2)	82.37(7)	P(3)−Au(3)−Au(4)	88.04(8)
S(1)−Au(1)−Au(2)	101.29(8)	S(5)−Au(3)−Au(4)	94.83(8)
P(2)−Au(2)−S(3)	168.89(11)	P(4)−Au(4)−S(7)	170.10(12)
P(2)−Au(2)−Au(1)	93.00(7)	P(4)−Au(4)−Au(3)	83.48(8)
S(3)−Au(2)−Au(1)	86.03(8)	S(7)−Au(4)−Au(3)	87.13(9)
N(1)−C(1)−S(2)	122.3(8)	N(3)−C(70)−S(6)	121.1(10)
N(1)−C(1)−S(1)	116.5(9)	N(3)−C(70)−S(5)	118.5(10)
S(2)−C(1)−S(1)	121.1(7)	S(6)−C(70)−S(5)	120.4(8)
N(2)−C(2)−S(4)	121.9(9)	N(4)−C(71)−S(8)	122.6(10)
N(2)−C(2)−S(3)	117.7(9)	N(4)−C(71)−S(7)	115.7(11)
S(4)−C(2)−S(3)	120.4(7)	S(8)−C(71)−S(7)	121.7(9)

which in both cases indicates metal−metal interaction. The diphosphine adopts a cis conformation, with torsion angles Au(1)−P(1)···P(2)−Au(2) = −20.8° and Au(3)−P(3)···P(4)−Au(4) = 24.5° that show that the two P−Au−S moieties in each molecule are slightly twisted with respect to each other. The cis conformation is usually preferred to the trans conformation as a result of the formation of Au−Au interactions. Only with bulky ligands such as 2,4,6-tris(trifluoromethyl)phenyl has the trans conformation been observed, with an intramolecular Au−Au distance of 7.041 Å.[22] There are no short gold−gold intermolecular contacts, and the shortest Au/Au intermolecular distance is 6.544 Å. The Au−P bond distances (2.247(3)−2.254(3)) are typical for this type of complex, as found also for **3** and **4**. The Au−S bond distances are similar (from 2.322(3) to 2.335(3)), comparable to those found in **3** and **4**, and slightly shorter than in complex **2**. The dithiocarbamate ligands are essentially monodentate, with Au−S distances of 3.135, 3.022, 3.075, and 3.265 Å respectively for each gold center and the corresponding second sulfur atom. As observed also for derivatives **3** and **4**, there are two slightly different C−S bond lengths (one shorter at 1.662(13)−1.690(14) Å and one longer at 1.712(13)−1.758(11) Å) and one short C−N bond length (1.324(12)−1.358(17) Å).

Crystal Structure of [Au($S_2CNC_{10}H_{20}O_4$)(CN(2,6-$Me_2C_6H_3$))] (8). Although with higher than usual error, due to the low quality of the crystals, the structure of **8** was established by X-ray diffraction and is shown in Figure 5, with selected bond lengths and angles in Table 5. The molecule crystallizes forming pairs with a second identical molecule in an anti configuration, at a short Au···Au distance of 3.565 Å. Each gold atom has three other neighbor gold atoms at *ca.* 7.50 Å. The C(1)−Au(1)−S(1) angle of 161.0(5)° corresponds to a gold coordination more distorted

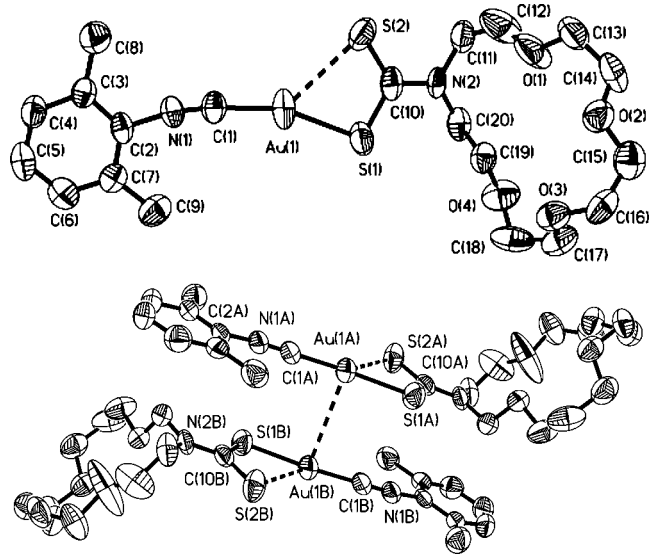

Figure 5. (Top) Structure of complex **8**, showing displacement ellipsoids at the 50% probability level (H atoms omitted for clarity). (Bottom) Dimer formed by short gold−gold intermolecular interactions.

Table 5. Selected Bond Lengths [Å] and Angles [deg] for Complex **8**

Au(1)−S(1)	2.352(4)	C(1)−Au(1)−S(1)	161.0(5)
Au(1)−C(1)	1.936(15)	N(1)−C(1)−Au(1)	172.3(14)
C(1)−N(1)	1.136(17)	C(1)−N(1)−C(2)	168.2(15)
N(1)−C(2)	1.412(17)	C(10)−S(1)−Au(1)	96.8(5)
S(1)−C(10)	1.740(16)	N(2)−C(10)−S(2)	123.5(12)
S(2)−C(10)	1.672(16)	N(2)−C(10)−S(1)	117.6(12)
C(10)−N(2)	1.343(17)	S(2)−C(10)−S(1)	118.8(8)
N(2)−C(11)	1.490(19)	C(10)−N(2)−C(11)	120.2(13)

from linear than for the previous derivatives (168.89(11)−176.31(10)°). The Au(1)−S(1) distance is longer than in complex **2** but similar to those found in derivatives **3**–**5**. Moreover, it displays a Au(1)−S(2) distance of 2.968 Å, close to that observed for the derivative with PPh_3. This again suggests that the dithiocarbamate ligand is essentially monodentate, but some weak S···Au interaction is not discarded. The Au(1)−C(1) and C(1)−N(1) distances are normal.[23]

Factors Controlling the Nuclearity of the Products. It is interesting to analyze why the chemical system constituted by a gold(I) center, a neutral ligand, and an (aza-15-crown-5)dithiocarbamate anion can give rise to three different results: a homoleptic dimer (**1**), a homoleptic hexanuclear compound (**2**), and heteroleptic mononuclear complexes (**3** and **4**). The dinuclear isomer, **1**, was obtained by displacement of a thioether (SMe_2,[13] or tht) from a putative intermediate **A** formed in situ by metathesis with the sodium salt of (aza-15-crown-5)dithiocarbamate (Scheme 2). The formation of **1** versus **A** is favored for a number of reasons: The overall increase in entropy, the gain in S−C−S resonance, and the volatility of the free thioether, which can be total or partially pumped off during evaporation of the solvent. In contrast, ligands with a higher Au−L bond energy, such as phosphines, maintain the monomeric structure **A**.

The reasons leading to the hexanuclear derivative **2** are less obvious. In fact, the isomerization of **1** to **2** is

(21) Wijnhoven, J. G.; Bosman, W. J. P. H.; Beursken, P. T. *J. Cryst. Mol. Struct.* **1972**, *2*, 7.
(22) Bardají, M.; Jones, P. G; Laguna, A.; Moracho, A.; Fischer, A. K. *J. Organomet. Chem.* **2002**, *648*, 1.
(23) Coco, S.; Cordovilla, C.; Espinet, P.; Martín-Álvarez, J. M.; Muñoz, P. *Inorg. Chem.* **2006**, *45*, 10180.

Scheme 2

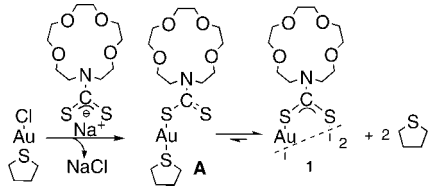

Scheme 3

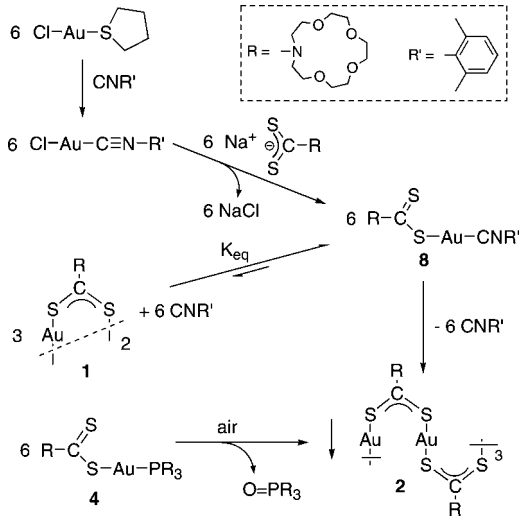

entropically disfavored, and experimentally, **1** in solution does not isomerize to **2**. Complex **2** was first obtained serendipitously according to Scheme 1, while trying to prepare the monomeric derivative **8**. It is known that chloro isocyanide complexes are easily obtained by ligand displacement from the corresponding tht precursors;[24] therefore, isocyanides are much better ligands for gold(I) than tht. The question is then: why and when is **2** formed, and not **1** or **8**?

The reaction of [AuClCNR] with sodium (aza-15-crown-5)dithiocarbamate was monitored by IR spectroscopy. The starting material, [AuClCNR], showed a ν(C≡N) band at 2214 cm^{-1}. Five minutes after adding the dithiocarbamate salt, two bands were observed at 2122 (free isocyanide) and 2197 cm^{-1}. The latter band is assigned to [Au(S_2CN-crown)(CNR)] **8**, and therefore we propose (Scheme 3) an equilibrium in solution of **8** and **1** (soluble), plus free isocyanide, plus **2** in unobservable concentration (it is practically insoluble).[25] Crystallization of this mixture afforded yellow microcrystals of the insoluble pure complex **2** in good yield, which points to a shift of the equilibrium due to the crystallization of **2** when the solubility limit of **2** (very low) is reached before those of **1** or **8** (comparatively high).

The reaction of **1** with isocyanide, monitored by IR spectroscopy, afforded the same equilibrium mixture, from which microcrystals of derivative **2** were also obtained (identified by X-ray diffraction). However, some crystals of **8** could be obtained from these solutions (mixed with crystals of **2**) when a large excess of isocyanide was added to prevent extensive crystallization of **2** (see Experimental Section). The crystals of **8** could be picked up from the mixture, and this made the unambiguous identification of **8** possible.

Assuming that integration of ν(C≡N) in solution is a reasonable measure of concentration, the equilibrium constant in Scheme 3 is $K_{eq} = 2[CN_{coord}]^2/[CN_{free}]^3 = 2.7 \times 10^4\ M^{-1}$. This approximate value affords concentrations of CN_{coord} and CN_{free} in the NMR solution at the same order of magnitude (e.g., 9×10^{-2} M in CNR gives 91% coordinated CNR), which should make the NMR of **8** observable. However, as the ^{1}H chemical shifts of the signal of the isocyanide hardly move from free to coordinated, the ^{1}H NMR spectra results are uninformative in detecting this reaction. Hexanuclear **2** can be equally prepared using other isocyanides. It was also formed when a solution of derivative **4** was left to evaporate slowly (several months). This led to a yellow powder containing **4**, triphenylphosphine oxide (by ^{31}P NMR), and yellow microcrystals of **2** (by X-ray diffraction) as shown in Scheme 3.

Complex **2** is insoluble once it is formed and does not dissolve to revert to **1** with thioethers, but it is solubilized in the presence of PPh_3 to give **4** or, slowly, in the presence of a large excess of CNR (R = 2,6-$Me_2C_6H_3$NC), to give the equilibrium of **2** and **8** discussed above.

In order to asses whether this reaction depends on the specific features of the crown dithiocarbamate, the reaction of [AuCl(CNR)] with other dithiocarbamates that are known to give well-characterized dinuclear derivatives was studied, affording only the corresponding dinuclear complex [$Au_2(S_2CNR'_2)_2$] (R′ = Et, *n*-pentyl).[26,12] This confirms that the presence of the crown ether is critical for the formation of **2**.

In view of all these results, the following observations seem to be apparent: (*i*) The formation of **1** is favored by the use of weak ligands (thioethers) because these are totally dissociated in solution, and the equilibrium mononuclear/**1** is totally displaced toward **1** at any concentration of the solution. Since this will not change noticeably upon evaporation (except favoring the displacement toward **1**, if the ligand is volatile), the only species virtually existing in the solution, **1**, will crystallize when its solubility limit is reached. (*ii*) Strong ligands (such as PPh_3), keeping the dissociation equilibrium totally displaced toward the monomer at any concentration (e.g., ratio **4**/**1** very high at all concentrations), will prevent the formation of any significant concentration of **1** or **2**, and the monomer will crystallize. (*iii*) Ligands of moderate strength (CNR) produce **1**, free CNR, and **8** in equilibrium, with not very disparate concentrations of each of them. Because of the mathematical expression of the dissociation constant, as the overall concentration in total gold of the solution increases, the equilibrium is less and less displaced toward **1**, preventing early saturation in **1**. The solubility of **2** being extremely low and the solubilities of **8**

(24) Benouzzane, M.; Coco, S.; Espinet, P.; Martín-Álvarez, J. M. *J. Mater. Chem.* **1995**, *5*, 441.

(25) A similar equilibrium does not operate for [AuClCNR)], which does not dissociate isocyanide. This shows that the ligand (crownNCS$_2$)$^-$ labilizes the bond of the isocyanide to Au(I). Probably some weak interaction of the appended sulfur with gold (in a three-coordinated complex) helps this labilization.

(26) Hong, M.-C.; Lei, X.-J.; Huang, Z.-Y. *Chin. Sci. Bull.* **1993**, *38*, 912.

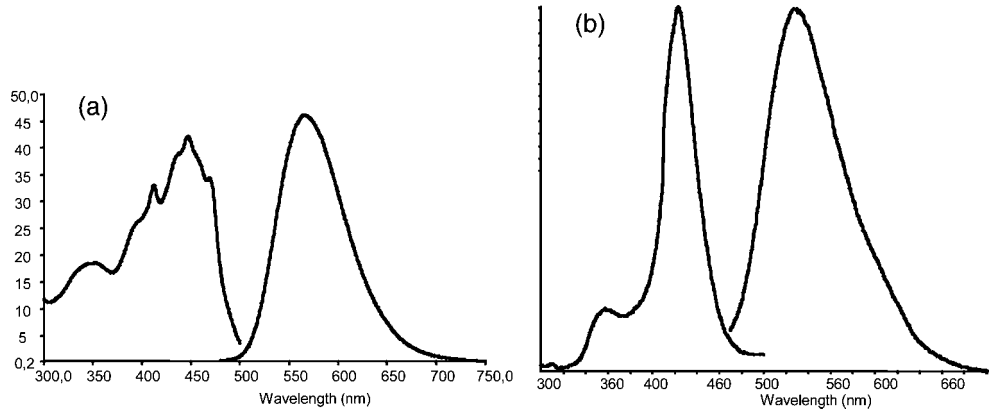

Figure 6. Excitation and emission spectra at 77 K in the solid state: (a) complex **2** and (b) complex **4**.

Table 6. Excitation and Emission Data for **1**−**5** and **8** in the Solid State

	298 K		77 K	
complex	λ_{exc}/nm	λ_{emis}/nm	λ_{exc}/nm	λ_{emis}/nm
1			355sh, 413, 447[a]	570
2	475,[a] 491	569	353sh, 412, 447,[a] 469	566
3			346sh, 411, 438, 451[a]	562
4			357, 423[a]	528
5			442	605
8			350, 414, 424,[a] 431	563

[a] Most intense peak.

Table 7. Extraction Efficiency of Derivatives **3**−**7**

extractor	% extracted[a,b]	% extracted (time)
3	25	41 (80 min)
4	69	79 (80 min)
5	76	99 (30 min)
6	78	94 (45 min)
7	73	96 (15 min)
4[c]	45[c]	50[c] (80 min)
7[c]	84[c]	96[c] (15 min)

[a] Measured after 5 min. [b] Calculated as follows: $(A_o - A)/A_o \times 100$; A_o = starting absorbance; A = final absorbance. [c] Data for potasium picrate (extractor concentration is half that of the sodium picrate experiments).

and **1** higher, and having shown that CNR is not so efficient at dissolving **2**, it is perfectly possible for the unobserved in solution **2** to be the first to become saturated and, therefore, the first that crystallizes. Only a high excess of CNR prevents, in part, this preference and leads to conditions where **8** and **2** crystallize together. (*iv*) Finally, starting from a concentrated solution of a complex with a strong ligand (e.g., **4**, with L = PPh_3), if the strong ligand is slowly removed (e.g., by oxidation to give a weak ligand $OPPh_3$ unable to dissolve **2**), crystallization of the insoluble **2** at that high concentration of total gold is favored, as observed.

Photophysical Studies. The solid-state emission and excitation spectra of the isolated complexes were determined at 298 and 77 K. The results are summarized in Table 6, and the spectra of complexes **2** and **4** are shown in Figure 6. Neither the dithiocarbamate ligand nor derivatives **6** and **7** emit. Complex **2** shows a weak emission at 298 K (in contrast with the reported non-emissive character of **1** at room temperature),[13] and an intense photoluminescence at 77 K. The emission maximum at *ca.* 565 nm does not change with the temperature, while the excitation maxima are blue-shifted upon lowering the temperature. For comparison, the emission spectra of **1** were measured at low temperatures, and it was found that it emits at wavenumbers very close to those of **2**. The spectra of **3** at 77 K are quite similar to those of **1** and **2**, while those of **4** are clearly blue-shifted, and the emission spectrum of **5** is red-shifted. The spectra of derivative **8** are very close to those of **1**−**3**.

The emission observed in gold(I) thiolate complexes has been assigned as a S(π) to Au(6p) ligand-to-metal charge transfer (LMCT). The presence of Au···Au interactions strongly influences the emission bands, which become LMMCT in nature,[4,27] although multiple state emissions (MC, LMCT, and LMMCT) have been proposed to explain the spectral behavior of dialkyldithiophosphonate dinuclear derivatives.[28] The presence of Au···Au interactions in **1** and **2** does not change the emission wavelength, although for complex **2**, it facilitates the emission (it is the only product to emit at room temperature). Moreover, the emission maxima are quite similar to those observed for derivatives **3** and **8**. Therefore, the emission measured for complexes **1**−**3** and **8** can be assigned to LMCT transitions. The emission of **4** can also be assigned as LMCT transitions mixed with a LLCT transition due to the presence of the phenyl rings in the ligands, as reported for other derivatives.[29] The red shift found for **5** is typically observed when going from a LMCT to a LMMCT transition.

Extraction Experiments. Except for the insoluble compound **2**, measurements were carried out on the extraction efficiency of sodium picrate from aqueous solutions by solutions of compounds **3**−**7** in dichloromethane (Table 7; see also Experimental Section). The results show that the three diphosphino complexes are clearly better and faster extractors than the two monophosphino derivatives. Looking at the X-ray structure of **5**, where the crown ethers are brought close in the space by the Au···Au bond, these results strongly suggest that the two crown ethers in **5**−**7** are cooperating to bind the cation in a chelating way, although probably not involving all the oxygen atoms of each crown. In other words, in a way very similar to the well-known chelate and macrocyclic effects, the coordination process of

(27) Mohamed, A. A.; Kani, I.; Ramirez, A. O.; Fackler, J. P., Jr. *Inorg. Chem.* **2004**, *43*, 3833.
(28) Lee, Y. A.; McGarrah, J. E.; Lachicotte, R. J.; Eisenberg, R. *J. Am. Chem. Soc.* **2002**, *124*, 10662.
(29) Bardají, M.; Calhorda, M. J.; Costa, P. J.; Jones, P. G.; Laguna, A.; Pérez, M. R.; Villacampa, M. D. *Inorg. Chem.* **2006**, *45*, 1059.

Table 8. Details of Crystal Data and Structure Refinement for Complexes **2**−**5** and **8**

compound	**2**	**3**	**4**	**5**	**8**
empirical formula	$C_{66}H_{120}Au_6N_6O_{24}S_{12}$	$C_{14}H_{29}AuNO_4PS_2\ CH_2Cl_2$	$C_{29}H_{35}AuNO_4PS_2$	$C_{47}H_{62}Au_2N_2O_8P_2S_4$	$C_{20}H_{29}AuN_2O_4S_2$
fw	2948.22	652.36	753.64	1367.10	622.54
temp (K)	298(2)	298(2)	298(2)	298(2)	298(2)
wavelength (Å)	0.71073	0.71073	0.71073	0.71073	0.71073
cryst syst	trigonal	monoclinic	triclinic	triclinic	monoclinic
space group	$R\bar{3}$	$P2(1)/n$	$P\bar{1}$	$P\bar{1}$	$P2(1)/c$
unit cell dim.: a (Å)	21.6188(14)	12.7845(15)	8.877(9)	16.241(5)	7.5764(16)
b (Å)	21.6188(14)	11.2682(14)	9.245(9)	16.904(5)	10.315(2)
c (Å)	17.116(2)	17.480(2)	19.55(2)	20.632(6)	29.397(6)
α (deg)	90	90	76.475(16)	77.470(5)	90
β (deg)	90	110.380(2)	78.053(16)	77.220(5)	92.202(4)
χ (deg)	120	90	81.773(17)	75.335(6)	90
vol. (Å^3)	6927.9(12)	2360.6(5)	1519(3)	5265(3)	2295.6(9)
Z	3	4	2	4	4
density (calc.) (Mg/m^3)	2.120	1.836	1.648	1.725	1.801
abs. coeff. (mm^{-1})	9.835	6.722	5.068	5.836	6.618
F(000)	4248	1280	748	2696	1224
cryst habit	prism	prism	prism	prism	plate
cryst size (mm)	0.06 × 0.06 × 0.06	0.32 × 0.23 × 0.18	0.23 × 0.14 × 0.08	0.34 × 0.23 × 0.12	0.40 × 0.38 × 0.07
Θ range for data colln.	1.61−23.26°	1.72−23.31°	2.18−23.18°	1.03−23.33°	2.09−23.32°
index ranges	$-24 \le h \le 14, -23 \le k \le 24, -19 \le l \le 18$	$-14 \le h \le 14, -12 \le k \le 12, -15 \le l \le 19$	$-9 \le h \le 9, -10 \le k \le 7, -21 \le l \le 21$	$-17 \le h \le 18, -15 \le k \le 18, -22 \le l \le 20$	$-8 \le h \le 8, -11 \le k \le 11, -32 \le l \le 32$
reflns collected	9418	10882	6552	24330	14851
ind. reflns	2177 [R(int) = 0.0673]	3412 [R(int) = 0.0244]	4179 [R(int) = 0.0430]	15080 [R(int) = 0.0380]	3334 [R(int) = 0.0497]
max. and min. trans.	1.000 and 0.651	1.000 and 0.622	1.000 and 0.283	1.000 and 0.414	1.000 and 0.387
data/restraints/param.	2177/0/202	3412/0/238	4179/0/344	15080/0/1132	3334/0/264
goodness-of-fit on F^2	0.872	1.049	1.031	1.013	1.040
final R indices [$I > 2\sigma(I)$]	R1 = 0.0330, wR2 = 0.0650	R1 = 0.0447, wR2 = 0.1220	R1 = 0.0680, wR2 = 0.1717	R1 = 0.0545, wR2 = 0.1268	R1 = 0.0776, wR2 = 0.1624
R indices (all data)	R1 = 0.0636, wR2 = 0.0721	R1 = 0.0515, wR2 = 0.1283	R1 = 0.0734, wR2 = 0.1803	R1 = 0.0972, wR2 = 0.1507	R1 = 0.0905, wR2 = 0.1713
larg. diff. peak hole (e.Å^{-3})	0.899 and −0.628	4.625 and −1.930	2.708 and −3.089	3.401 and −2.260	5.258 and −3.030

the three diphosphine complexes benefits from a lower unfavorable entropy contribution, because these gold complexes have the crown ethers prearranged for chelation. This effect is even sharper when the experiment is carried out with potassium picrate because, as expected, this cation will be more effectively extracted as a sandwich by 15-crown ethers. Actually, the dinuclear derivative **7** extracts K^+ better and faster than the mononuclear derivative **4**, and the difference is bigger than that for Na^+.

Experimental Section

General. All reactions were carried out under a N_2 atmosphere at room temperature. Spectroscopic and analytical data were obtained as reported elsewhere.[30]

Extraction Experiments. To a dichloromethane solution (10 mL) of the extracting gold compound (10^{-3} M in crown ether; 5×10^{-4} M in crown ether for the potasium experiments) was added an aqueous solution of sodium picrate (10 mL, 5×10^{-5} M) prepared in situ by mixing solutions of picric acid and sodium hydroxide. The mixture was vigorously stirred, and samples were taken every 5 min to monitor the diminution of sodium picrate concentration in the aqueous phase by UV–vis spectrophotometry ($\lambda = 356$ nm), until successive determinations showed no variation. This was taken as an indication that equilibrium had been reached.

Preparation of $[Au_6(S_2CNC_{10}H_{20}O_4)_6]$ (2). To a dichloromethane solution (10 mL) of [AuCl(CNR)] (R = 2,6-$Me_2C_6H_3$; 73 mg, 0.2 mmol)[24] was added $Na(S_2CNC_{10}H_{20}O_4)$ (63 mg, 0.2 mmol).[31] The solid dissolved rapidly. The resulting yellow solution was stirred for about 15 min and then filtered through kieselgur. Yellow crystals were obtained by slow diffusion of hexane into the dichloromethane solution, after standing at −18 °C. Yield of **2**: 64 mg, 65%. IR (KBr): 1483 ν(C═N), 991 ν(C−S) cm^{-1}. Anal. calcd for $C_{66}H_{120}Au_6N_6O_{24}S_{12}$: C, 26.89; H, 4.1; N, 2.85. Found: C, 26.84; H, 3.8; N, 2.82.

Preparation of $[Au(S_2CNC_{10}H_{20}O_4)(PR_3)]$ (R = Me, 3; Ph, 4). These derivatives were prepared in two different ways. Method **A**: To a dichloromethane solution (20 mL) of $[AuCl(PR_3)]$ (0.2 mmol; R = Me, 62 mg; Ph, 99 mg)[32] was added $Na(S_2CNC_{10}H_{20}O_4)$ (63 mg, 0.2 mmol). The white solid dissolved rapidly, and the resulting yellow solution was stirred for about 1 h and then filtered through kieselgur and concentrated to *ca.* 2 mL. The addition of diethyl ether (20 mL) afforded complexes **3** and **4** as yellow solids, which were washed with diethyl ether (2 × 5 mL). Method **B**: To a dichloromethane suspension of **1** or **2** (98 mg; 0.1 or 0.033 mmol, respectively) was added the corresponding amount of phosphine (0.2 mmol: PMe_3,15 mg; PPh_3, 52 mg). The resulting clear solution was stirred for 1 h and concentrated to *ca.* 2 mL. The addition of diethyl ether (20 mL) afforded complexes **3** and **4**. Yield of **3**: 73 mg, 65%. ^{1}H NMR: δ 1.59 (d, 9H, $^2J_{PH}$ = 10.5 Hz, Me), 3.65 (s, 12H, OCH_2CH_2O), 3.94 (t, 4H, $^3J_{HH}$ = 6.1 Hz, $OC\underline{H}_2CH_2N$), 4.15 (t, 4H, $OCH_2C\underline{H}_2N$). $^{31}P\{^1H\}$ NMR: δ −6.32 (s). IR (KBr): 1473 ν(C═N), 985, 965 ν(C−S) cm^{-1}. Anal. calcd for $C_{14}H_{29}AuNO_4PS_2$: C, 29.63; H, 5.15; N, 2.47. Found: C, 29.44; H, 4.81; N, 2.49. Yield of **4**: 102 mg, 68%. ^{1}H NMR: δ 3.64 (s, 12H, OCH_2CH_2O), 3.96 (t, 4H, $^3J_{HH}$ = 6.1 Hz, $OC\underline{H}_2CH_2N$), 4.17 (d, 4H, $OCH_2C\underline{H}_2N$), 7.39–7.63 (m, 15H, Ph). $^{31}P\{^1H\}$ NMR: δ 36.86 (s). IR (KBr): 1479 ν(C═N), 998, 987 ν(C−S) cm^{-1}. Anal. calcd for $C_{29}H_{35}AuNO_4PS_2$: C, 46.22; H, 4.68; N, 1.86. Found: C, 45.83; H, 4.34; N, 2.05.

Preparation of $[(\mu\text{-P-P})\{Au(S_2CNC_{10}H_{20}O_4)\}_2]$ (P-P = dppm, 5; dppp, 6; dppf, 7). To a dichloromethane solution (20 mL) of [AuCl(tht)][33] (64 mg, 0.2 mmol) was added $Na(S_2CNC_{10}H_{20}O_4)$ (64 mg, 0.2 mmol). The yellow solution was stirred for about 1 h and filtered through kieselgur. Then, the bisphosphine was added (0.1 mmol; P-P = 38.5 mg dppm, 41 mg dppp, 57 mg dppf). The solution was stirred for about 30 min, and the solvent was evaporated. The residue was washed with diethyl ether (3 × 5 mL) to afford the corresponding complexes as yellow (**5** and **6**) or orange (**7**) solids. Yield of **5**: 112 mg, 82%. ^{1}H NMR: δ 3.65 (s, 26H, OCH_2CH_2O and PCH_2P), 3.97 (t, 8H, $^3J_{HH}$ = 5.7 Hz, $OC\underline{H}_2CH_2N$), 4.20 (brs, 8H, $OCH_2C\underline{H}_2N$), 7.24–7.74 (m, 20H, Ph). $^{31}P\{^1H\}$ NMR: δ 28.9 (s). IR (KBr): 1467 ν(C═N), 998, 989 ν(C−S) cm^{-1}. Anal. calcd for $C_{47}H_{62}Au_2N_2O_8P_2S_4$: C, 41.29; H, 4.57; N, 2.05. Found: C, 41.69; H, 4.3; N, 2.14. Yield of **6**: 68 mg, 50%. ^{1}H NMR: δ 2.10 (m, 2H, $PCH_2C\underline{H}_2CH_2P$), 2.88 (m, 4H, $PC\underline{H}_2CH_2C\underline{H}_2P$), 3.66 (s, 24H, OCH_2CH_2O), 3.97 (t, 8H, $^3J_{HH}$ = 6.15 Hz, $OC\underline{H}_2CH_2N$), 4.19 (t, 8H, $^3J_{HH}$ = 6.15 Hz, $OCH_2C\underline{H}_2N$), 7.40–7.83 (m, 20H, Ph). $^{31}P\{^1H\}$ NMR: δ 29.3 (s). IR (KBr): 1467 ν(C═N), 998, 987 ν(C−S) cm^{-1}. Anal. calcd for $C_{49}H_{66}Au_2N_2O_8P_2S_4$: C, 42.18; H, 4.77; N, 2.01. Found: C, 41.84; H, 4.57; N, 1.72. Yield of **7**: 109 mg, 71%. ^{1}H NMR: δ 3.66 (s, 24H, OCH_2CH_2O), 3.98 (t, 8H, $^3J_{HH}$ = 6.2 Hz, $OC\underline{H}_2CH_2N$), 4.19 (t, 8H, $^3J_{HH}$ = 6.2 Hz, $OCH_2C\underline{H}_2N$), 4.28 (t, 4H, $^3J_{HP}$ = 3.3 Hz, P−C−CH in Cp), 4.85 (brs, 4H, P−C−CH−C$\underline{H}$ in Cp), 7.34–7.59 (m, 20H, Ph). $^{31}P\{^1H\}$ NMR: δ 30.4 (s). IR (KBr): 1468 ν(C═N), 997, 987 ν(C−S) cm^{-1}. Anal. calcd for $C_{56}H_{68}Au_2FeN_2O_8P_2S_4$: C, 43.76; H, 4.46; N, 1.82. Found: C, 43.38; H, 3.98; N, 2.09.

Preparation of $[Au(S_2CNC_{10}H_{20}O_4)(CNR)]$ (R = 2,6-$Me_2C_6H_3$, 8). To a dichloromethane solution (5 mL) of [AuCl(CNR)] (62 mg, 0.17 mmol) was added $Na(S_2CNC_{10}H_{20}O_4)$ (54 mg, 0.17 mmol). The solid dissolved rapidly, and the resulting yellow solution was stirred for about 15 min and then filtered through kieselgur. The clear solution was concentrated to ca. 1 mL, from which yellow crystals were obtained by slow diffusion of 10 mL of a hexane solution of 0.05 M isocyanide (molar ratio of dithiocarbamate/CNR 1:4), after standing at −18 °C. Two differently shaped crystals were found: cubes, corresponding to compound **2**, and plates, corresponding to compound **8**. The latter were selected by hand for X-ray diffraction and to record an FTIR spectrum. IR (KBr): 2179 ν(C≡N).

Crystal Structure Determination of 2–5 and 8. The crystals were mounted on glass fibers and transferred to a Bruker SMART CCD diffractometer. Cell parameters were retrieved using SMART[34] software and refined with SAINT[35] on all observed reflections. Data reduction was performed with the SAINT software and corrected for Lorentz and polarization effects. Absorption corrections were based on multiple scans (program SADABS).[36] The structures were solved by direct methods and refined anisotropically on F^2.[37] All non-hydrogen atomic positions were located in difference Fourier maps

(30) Arias, J.; Bardají, M.; Espinet, P. *J. Organomet. Chem.* **2006**, *691*, 4990.
(31) Granell, J.; Green, M. L. H.; Lowe, V. J.; Marder, S. R.; Mountford, P.; Saunders, G. C.; Walker, N. M. *J. Chem. Soc., Dalton Trans.* **1990**, 605.
(32) Schmidbaur, H.; Wohlleben, A.; Wagner, F.; Orama, O.; Huttner, G. *Chem. Ber.* **1977**, *110*, 1748.
(33) Usón, R.; Laguna, A.; Laguna, M. *Inorg. Synth.* **1989**, *26*, 85.
(34) *SMART V5.051, software for the CCD Detector System*; Bruker Analytical X-ray Instruments Inc.; Madison, WI, 1998.
(35) *SAINT V6.02, integration software*; Bruker Analytical X-ray Instruments Inc.; Madison, WI, 1999.
(36) Sheldrick, G. M. *SADABS: A program for absorption correction with the Siemens SMART system*; University of Göttingen: Göttingen, Germany, 1996.
(37) *SHELXTL program system*, version 5.1; Bruker Analytical X-ray Instruments Inc.; Madison, WI, 1998.

and refined anisotropically, with some exceptions for derivative **5** (see below). The hydrogen atoms were placed in their geometrically generated positions. Crystal data and details of data collection and structure refinement are given in Table 8. In complex **2**, the atoms O2, O3, and C9 are disordered in two positions, with the following occupancy: O2A = 0.33(7), O3A = 0.32(5), and C9A = 0.65(4); only the major component is shown in the figures. The structure of **3** is a solvate with disordered dichloromethane. The highest residual density peak is very close to the gold center. In complex **4**, there are high residual density peaks very close to the gold center. The structure of **5** shows high residual density peaks very close to the four independent gold centers. Moreover, two flapping crown ethers have been solved by considering the atoms O6, C18, C78, and O11 as disordered (they are not refined anisotropically) in two positions with the following occupancy: O6A = 0.55(5), C18A = 0.41(7), C78A = 0.58(8), and O11A = 0.40(6); the third ring was refined as a rigid group. In complex **8**, there is a high residual density peak very close to the gold center.

Acknowledgment. We thank the Spanish Comisión Interministerial de Ciencia y Tecnología (Project CTQ2005-08729) and the Junta de Castilla y León (Project VA099A05) for financial support. J.A. thanks the Ministerio de Edución y Ciencia (Spain) for a grant. We also thank Dr. J. M. Martín-Alvarez for taking X-ray data of complex **2** and Dr. D. Miguel for structural discussions.

Supporting Information Available: A crystallographic information file (CIF) containing structural data for **2**−**5** and **8** is provided. This material is available free of charge via the Internet at http://pubs.acs.org.

IC702252J